JACC: CARDIOVASCULAR IMAGING VOL. 5, NO. 8, 2012

ISSN 1936-878X/$36.00
PUBLISHED BY ELSEVIER INC. http://dx.doi.org/10.1016/j.jcmg.2011.12.024

# MR Cine DENSE Dyssynchrony Parameters for the Evaluation of Heart Failure

## Comparison With Myocardial Tissue Tagging

Loren P. Budge, MD,* Adam S. Helms, MD,* Michael Salerno, MD, PhD,* Christopher M. Kramer, MD,* Frederick H. Epstein, PhD,† Kenneth C. Bilchick, MD, MS*

*Charlottesville, Virginia*

**OBJECTIVES** We sought to assess the effectiveness of automated mechanical dyssynchrony (MD) parameters based on regional heterogeneity of strain (circumferential [CURE], longitudinal [LURE], and radial uniformity ratio estimates) relative to parameters based on regional time to peak contraction with cardiac magnetic resonance (CMR) cine DENSE (Displacement Encoding with Stimulated Echoes) validated with myocardial tissue tagging (MTT) strain data.

**BACKGROUND** Dyssynchrony measures based on the Fourier transformation (FT) of regional strain, such as CURE (previously evaluated in cardiac resynchronization therapy candidates), directly assess MD and yield straightforward global dyssynchrony indexes; however, performance relative to the 12-segment standard deviation of time to peak strain (SD12) or maximal regional delay in time to peak strain is unknown.

**METHODS** Cine DENSE and MTT were obtained with CMR (1.5-T Siemens Avanto, Siemens, Erlangen, Germany) in 13 canines: 3 normal control subjects, 5 with tachycardia pacing-induced heart failure (HF) and left bundle branch ablation (LBBB-HF), and 5 with HF and narrow QRS (NQRS-HF). Strain and dyssynchrony parameters were determined with both CMR methods.

**RESULTS** Both HF groups had reduced peak strains and left ventricular ejection fraction compared with normal cases. There was strong agreement between cine DENSE and MTT on the basis of intraclass correlation coefficients (CURE: 0.99, 95% CI: 0.96 to 1.00; LURE: 0.92, 95% CI: 0.77 to 0.98; circumferential strain [$E_{CC}$]: 0.95, 95% CI: 0.72 to 0.99; longitudinal strain [$E_{LL}$]: 0.82, 95% CI: 0.42 to 0.97). The FT-based metrics (scale 0 to 1), in particular CURE, discriminated highly between LBBB-HF and NQRS-HF groups (median difference): CURE: 0.60, 95% CI: 0.43 to 0.76; LURE: 0.39, 95% CI: 0.19 to 0.58; radial uniformity ratio estimate: 0.22, 95% CI: 0.04 to 0.40). In contrast, relative confidence intervals for group differences in time-to-peak parameters were wide, indicating less consistent discrimination (median difference): SD12-$E_{CC}$: 52.5, 95% CI: −4.0 to 109.2; SD12-$E_{LL}$: 40.9, 95% CI: −5.3 to 87.1; SD12-radial strain: 42.0, 95% CI: 0.4 to 83.6). Correlations between FT-based and time-to-peak parameters were significant (CURE/SD12-$E_{CC}$: $r = -0.62$, $p = 0.03$; LURE/SD12-$E_{LL}$: $r = -0.76$, $p = 0.005$) but not as tight as correlations between time-to-peak parameters.

**CONCLUSIONS** Automated FT-based circumferential, radial, and longitudinal dyssynchrony measures compare favorably with time-to-peak parameters. Cine DENSE was effective for this application and validated with MTT. Further clinical evaluation in cardiac resynchronization therapy candidates with CMR or other imaging modalities is warranted. (J Am Coll Cardiol Img 2012;5:789–97) © 2012 by the American College of Cardiology Foundation

From the *Department of Medicine, University of Virginia Health System, Charlottesville, Virginia; and the †Department of Biomedical Engineering, University of Virginia Health System, Charlottesville, Virginia. This work was supported by National Institutes of Health Grants K23 HL094761 (to Dr. Bilchick) and R01 EB001763 (to Dr. Epstein). Drs. Salerno, Kramer, and Epstein have received grant support from Siemens. Dr. Kramer is a consultant for St. Jude Medical. Pacemakers designated for animal use were donated by St. Jude Medical. All other authors have reported that they have no relationships relevant to the contents of this paper to disclose. Drs. Budge and Helms contributed equally to this work. Warren Manning, MD, served as Guest Editor for this paper.

Manuscript received September 12, 2011; revised manuscript received November 16, 2011, accepted December 13, 2011.

The overall benefit of cardiac resynchronization therapy (CRT) to selected patients with heart failure (HF) has been shown in clinical trials (1–4), but the nonresponse rate to CRT with current clinical indications is still significant at approximately 30% to 40% (5). Although other biological factors are involved in CRT response (6), cardiac imaging remains the best-studied tool to achieve more accurate identification of CRT responders. Even so, a number of early mechanical dyssynchrony parameters were unable to identify CRT responders effectively in a multicenter clinical trial (5). Although these results have led some to question whether cardiac imaging can identify patients most likely to respond to CRT, an alternative response has been to look for more effective imaging techniques and approaches for CRT patients. For example, there have been promising results shown for echo speckle tracking (7), 3-dimensional (3D) echo (8), and cardiac magnetic resonance (CMR) with myocardial tissue tagging (MTT) (9). Magnetic resonance (MR) cine Displacement Encoding with Stimulated Echoes (DENSE) is another imaging approach with high potential. DENSE encodes tissue displacement directly into the phase of the MR signal (10), provides high spatial resolution, accurately assesses circumferential, longitudinal, and radial strain, provides rapid strain analysis (11), and offers automatic contouring (12) without the need for tag detection or a minimum tag density.

**ABBREVIATIONS AND ACRONYMS**

**CMR** = cardiac magnetic resonance

**CRT(-D)** = cardiac resynchronization therapy (defibrillator)

**CURE** = circumferential uniformity ratio estimate

$E_{CC}$ = circumferential strain

$E_{LL}$ = longitudinal strain

$E_{RR}$ = radial strain

**FT** = Fourier transformation

**HF** = heart failure

**LBBB** = left bundle branch block

**LURE** = longitudinal uniformity ratio estimate

**LV** = left ventricular

**LVEF** = left ventricular ejection fraction

**MTT** = myocardial tissue tagging

**NQRS** = narrow QRS

**RURE** = radial uniformity ratio estimate

**SD12** = standard deviation of time to peak strain in 12 segments

In addition to the imaging modality used, the parameterization of dyssynchrony is also an important factor. Widely used dyssynchrony parameters are based on time to peak contraction, indexed as the delay in opposing walls or standard deviation of time to peak strain in 12 segments (SD12) (7,13–15). Although associated studies have shown positive results, identification in peaks in tissue velocity or strain curves might be time-consuming, subjective, and very difficult (or impossible) for segments with infarction, akinesis, dyskinesis, or very low maximum contractile strain. An alternative approach (not specific to CMR) is the use of automated global circumferential (circumferential uniformity ratio estimate [CURE]) (9,16), radial (radial uniformity ratio estimate [RURE]), and longitudinal (longitudinal uniformity ratio estimate [LURE]) dyssynchrony indexes, which are based on the Fourier transformation (FT) of regional strain (FT-based parameters) and do not require assessment of regional strain or velocity peaks.

In the present study, we aimed to assess the hypotheses that FT-based parameters would perform better than corresponding timing-based parameters and that cine DENSE would be feasible and valid for this application on the basis of comparison with MTT. We elected to compare these indexes in a validated animal model of HF with and without left bundle branch block (LBBB) rather than in a human CRT study. Because HF with dyssynchrony modeled this way has been shown to improve with resynchronization (16), it was an ideal model to test our hypotheses. Although the study was implemented with CMR, the findings of this study may be extended to any imaging technique that can generate regional strain curves from standard short-axis and long-axis slices.

## METHODS

**Animal model.** Approval for the study was obtained through the University of Virginia Animal Care and Use Committee. As a validated model of dyssynchronous HF (17), we performed left bundle branch ablation (50 W, temperature ≤60°) before tachycardia pacing (LBBB-HF) with a 4-mm-tip ablation catheter in 5 canines, resulting in widening of the QRS duration from 55 to 60 ms to approximately 120 ms with a typical LBBB appearance. Persistence of LBBB was confirmed after a 30-min waiting period as well as at the time of final MR examination. Cardiomyopathy was induced in a total of 10 canines with right atrial tachy-pacing at 180 beats/min for 5 weeks (the 5 LBBB-HF animals, and 5 animals without left bundle ablation [NQRS-HF]). Three normal canines did not undergo ablation or tachy-pacing.

**CMR protocol.** With a 1.5T Avanto scanner (Siemens Medical Solutions, Erlangen, Germany) with a 4-channel phased-array chest radiofrequency coil, we performed cine DENSE imaging in standard short-axis and long-axis planes in two orthogonal directions for each plane with the following parameters (10,18): interleaved spiral readout with 6 interleaves/image; repetition time/echo time 17/1.9 ms; section thickness 8 mm; field of view 350 × 350 mm; flip angle 15°; pixel size 2.8 × 2.8 mm; fat suppression; echo spacing 17 ms with view sharing;

and displacement-encoding frequency 0.1 cycles/mm. The MTT images were obtained with a gradient echo grid tagging sequence: tag spacing 7 mm; repetition time/echo time 8.7/4.2 ms; slice thickness 8 mm; field of view 250 × 250 mm; flip angle 14°; pixel size 1.4 × 1.0 mm; and temporal resolution 17.5 ms with view sharing (19).

**Image analysis and calculation of dyssynchrony metrics.** After image acquisition, segmentation of the left ventricular (LV) myocardium was performed, a phase-unwrapping algorithm was applied to LV myocardium pixels, and displacements were calculated (11). Lagrangian strain was computed from displacements in 24 short-axis segments in multiple slices and then projected in both the radial ($E_{RR}$) and circumferential ($E_{CC}$) directions relative to the LV center of mass. Longitudinal strain ($E_{LL}$) was determined by analysis of strain in standard long-axis planes in basal and mid-cavity segments. Left ventricular volumes and ejection fraction were calculated from cine steady-state free precession images with Argus software. Strains were calculated from cine DENSE images with an algorithm developed in Matlab (MathWorks, Natick, Massachusetts) and from MTT images with harmonic phase analysis software (Diagnosoft, Inc., Cary, North Carolina) (11).

Dyssynchrony was assessed by 2 types of analyses for each strain component: variability in time to peak strain and the FT-based uniformity ratio estimates (CURE, LURE, and RURE). Basic timing delays for each strain component were calculated as the difference in time from QRS onset to peak strain for opposing LV segments with earliest and latest peak strain ($E_{CC}$-Delay, $E_{LL}$-Delay, and $E_{RR}$-Delay). The SD12-$E_{CC}$, SD12-$E_{LL}$, and SD12-$E_{RR}$ were constructed on the basis of the SD of time to peak strain in 6 basal and 6 mid-cavity segments (12 total segments) similar to the method Yu et al. (14) used for regional tissue velocity.

The CURE, LURE, and RURE were calculated as previously described (16). Briefly, this technique involves a simple and automated analysis on the basis of the FT of the spatial distribution of strain. Because synchronous contraction is represented primarily by zero-order FT terms and dyssynchronous contraction by first-order FT terms, a ratio measure involving these terms (the square root of the ratio of the zero-order term to the sum of zero and first-order terms) can be used to index dyssynchrony on a scale between 0 (dyssynchrony) and 1 (synchrony) (9).

**Statistical analysis.** The Wilcoxon rank sum test with exact p values was used to compare continuous variables, whereas the Hodges Lehmann estimate and exact 95% confidence interval (CI) were used to evaluate the median differences between groups. Boxplots were also constructed for a visual comparison of these differences between groups. For pairwise correlations, the Pearson correlation coefficient (r) and associated significance level are reported. Comparison between cine DENSE and MTT was performed with the intraclass correlation coefficients for absolute agreement between methods. Results are presented graphically with both scatter plots with regression lines and Bland-Altman plots. Statistical analysis was performed with SAS (version 9.2, SAS, Cary, North Carolina).

## RESULTS

**Animal model.** Successful left bundle branch ablations were completed in all LBBB-HF animals, with resulting QRS durations of 120 ms and characteristic LBBB morphology on the 12-lead electrocardiogram; QRS durations were 55 to 60 ms in the NQRS-HF group and control groups. After 5 weeks of tachy-pacing, all LBBB-HF and NQRS-HF group animals displayed LV dysfunction with left ventricular ejection fraction (LVEF) <0.30. The LBBB-HF group showed a trend for lower LVEF (median 0.15 vs. 0.24, $p = 0.14$) and had increased LV end-diastolic volumes (median 110 vs. 77 ml, $p = 0.008$) relative to the NQRS-HF group. Normal animals had a greater LVEF than HF animals (median 0.57 vs. 0.15, $p = 0.017$). Examples of CMR steady-state free precession and Lagrangian displacement movies for both an LBBB-HF case and NQRS-HF case may be found in Online Videos 1, 2, 3, and 4.

**Comparison of cine DENSE and MTT.** As shown in Figure 1, agreement between cine DENSE and MTT was excellent for peak $E_{CC}$ ($R^2 = 0.94$, $p < 0.01$; intraclass correlation coefficient [ICC] for absolute agreement between methods: 0.95, 95% CI: 0.72 to 0.99) and CURE ($R^2 = 0.98$, $p < 0.001$; ICC: 0.99, 95% CI: 0.96 to 1.00). There was also good agreement between DENSE and MTT for peak $E_{LL}$ (peak $E_{LL}$: $R^2 = 0.86$, $p < 0.01$; ICC: 0.82, 95% CI: 0.42 to 0.97) and LURE ($R^2 = 0.85$, $p < 0.001$; ICC: 0.92, 95% CI: 0.77 to 0.98) (Online Appendix). As previously reported, MTT-based radial strain and dyssynchrony measures were of insufficient precision to include in our analysis (20).

**Comparison between NQRS-HF and LBBB-HF groups.** The NQRS-HF and LBBB-HF animals had marked heterogeneity in regional strain curves (see

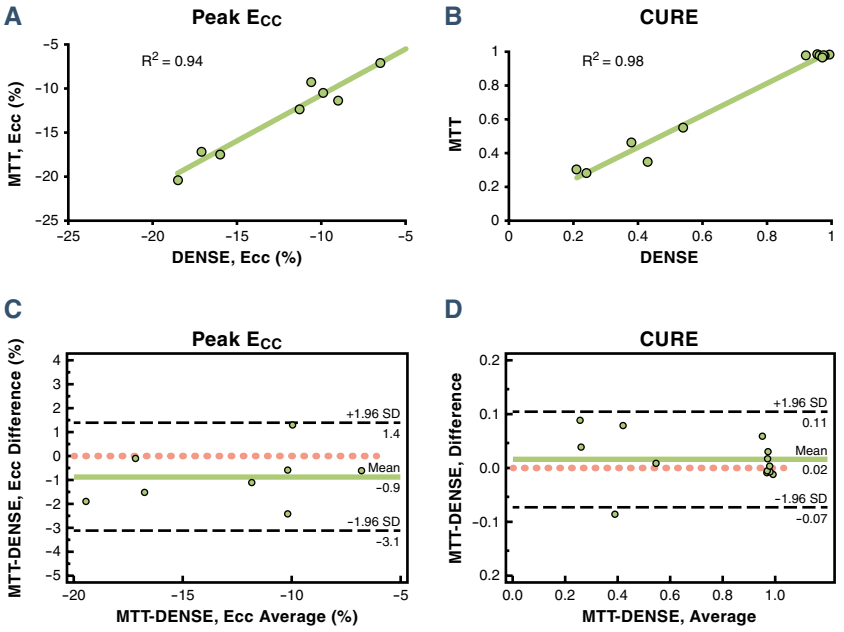


**Figure 1. Peak $E_{CC}$ and Circumferential Dyssynchrony From Cine DENSE versus MTT**

Correlation between cine Displacement Encoding with Stimulated Echoes (DENSE) and myocardial tissue tagging (MTT) is shown for **(A)** circumferential strain ($E_{CC}$) and **(B)** the circumferential dyssynchrony measure circumferential uniformity ratio estimate (CURE). Agreement between the methods is also shown in the form of Bland Altman plots for **(C)** $E_{CC}$ and **(D)** CURE.

Online Appendix for examples of circumferential, longitudinal, and radial regional strain curves for each group). Although the regional strain polarity (positive or negative) was generally the same regardless of the strain component for NQRS-HF animals, typical regional strain versus time curves for the LBBB-HF group show simultaneous positive and negative strains in different sectors. This indicates early anteroseptal contraction and lateral wall stretch, followed by late lateral wall contraction and anteroseptal stretch. Statistically significant differences in all FT-based parameters ($p < 0.01$ for CURE and LURE; $p = 0.016$ for RURE) are evident from Table 1, although the magnitude of the difference between LBBB-HF and NQRS-HF groups was greatest for CURE, followed by LURE and RURE (CURE: 0.60, 95% CI: 0.43 to 0.76; LURE: 0.39, 95% CI: 0.19 to 0.58; RURE: 0.22, 95% CI: 0.04 to 0.40).

Boxplots comparing FT-based metrics with corresponding timing-based dyssynchrony parameters (SD12 and opposing wall delay) are shown in Figures 2, 3, and 4 for circumferential, longitudinal, and radial parameters, respectively. From these boxplots, it is evident that although time-to-peak parameters indicate more dyssynchrony for

**Table 1. Differences Among Groups for CMR Dyssynchrony Parameters**

| | Median Difference for LBBB-HF vs. NQRS-HF, Midpoint (95% CI) | p Value | Median Difference for LBBB-HF vs. Normal, Midpoint (95% CI) | p Value |
|---|---|---|---|---|
| CURE (0–1) | 0.60 (0.43 to 0.76) | 0.008 | 0.60 (0.42 to 0.78) | 0.04 |
| LURE (0–1) | 0.39 (0.19 to 0.58) | 0.008 | 0.42 (0.23 to 0.61) | 0.04 |
| RURE (0–1) | 0.22 (0.04 to 0.40) | 0.016 | 0.40 (0.23 to 0.56) | 0.04 |
| SD12-$E_{CC}$ (ms) | 52.5 (−4.0 to 109.2) | 0.09 | 57.8 (−3.5 to 119.1) | 0.07 |
| SD12-$E_{LL}$ (ms) | 40.9 (−5.3 to 87.1) | 0.19 | 46.4 (1.1 to 91.6) | 0.05 |
| SD12-$E_{RR}$ (ms) | 42.0 (0.4 to 83.6) | 0.03 | 58.8 (12.1 to 105.5) | 0.04 |
| $E_{CC}$-Delay (ms) | 93.5 (−17 to 204) | 0.09 | 85.0 (−17 to 187) | 0.25 |
| $E_{LL}$-Delay (ms) | 93.5 (−51 to 238) | 0.25 | 127.0 (−17 to 272) | 0.31 |
| $E_{RR}$-Delay (ms) | 42.5 (−51 to 136) | 0.20 | 110.5 (0 to 221) | 0.11 |

CI = confidence interval; CMR = cardiac magnetic resonance; HF = heart failure; LBBB = left bundle branch block; NQRS = narrow QRS.

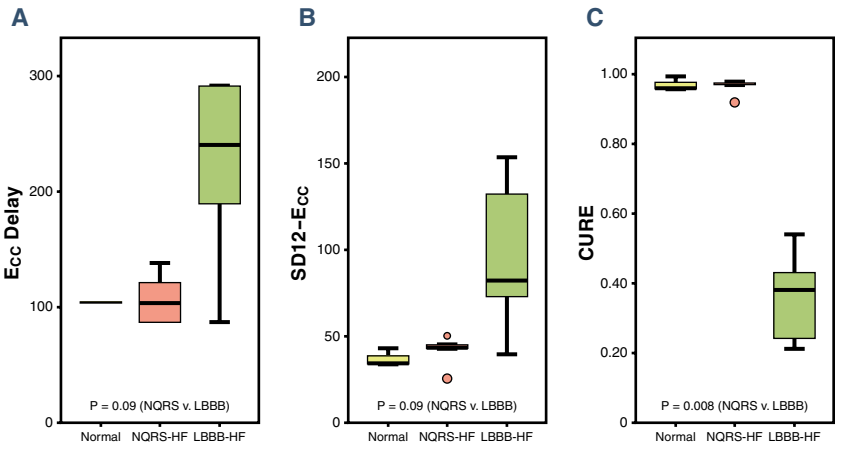


**Figure 2. Boxplots of Circumferential Dyssynchrony Parameters**

A boxplot comparison of (**A**) circumferential strain ($E_{CC}$)-Delay, (**B**) SD12-$E_{CC}$, and (**C**) circumferential uniformity ratio estimate (CURE) in normal, narrow QRS (NQRS-HF), and left bundle branch ablation (LBBB-HF) groups is shown.

LBBB-HF relative to NQRS-HF cases, the time-to-peak parameters are less consistent within each group (relative to FT-based parameters). The less consistent discrimination with time-to-peak parameters is also apparent from Table 1, which shows that even time-to-peak parameters based on 12 segments have much wider CIs (relative to the scale of the parameter) for the median differences between the LBBB-HF and NQRS-HF groups (SD12-$E_{CC}$: 52.5, 95% CI: −4.0 to 109.2; SD12-$E_{LL}$: 40.9, 95% CI: −5.3 to 87.1; SD12-$E_{RR}$: 42.0, 95% CI: 0.4 to 83.6).

The 2 LBBB-HF cases in Figure 5 both have significant dyssynchrony and illustrate some of the advantages of FT-based parameters. In panel A, the circumferential and radial strain curves show absent early septal contraction (sometimes seen when LV systolic dysfunction is more severe or infarction is present). The CURE and RURE still both correctly indicate significant dyssynchrony, but time-to-peak measures do not because there are no early contractile strain peaks. There is better agreement in dyssynchrony assessments in panel B, which shows the classic pattern of early septal contraction and early free wall stretch followed by late free wall contraction and late septal stretch.

**Comparison between normal and HF groups.** Figures 2, 3, and 4 also show comparisons for all 9 dyssynchrony parameters between normal cases and those with HF. Dyssynchrony parameters in the normal

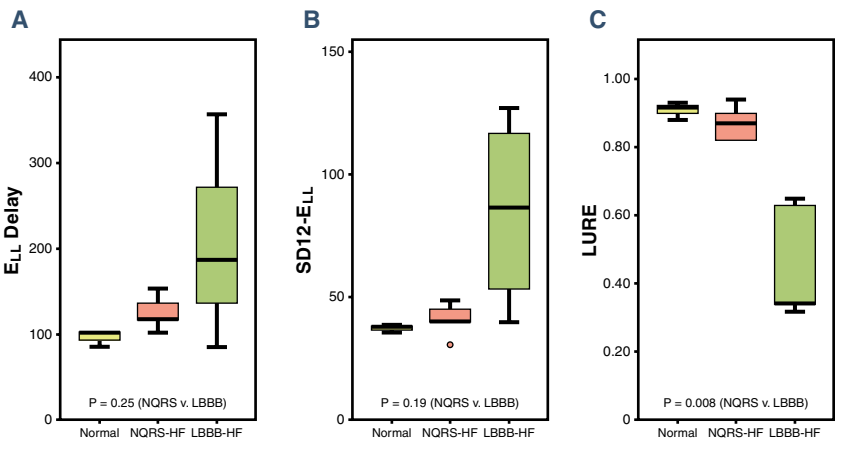


**Figure 3. Boxplots of Longitudinal Dyssynchrony Parameters**

A boxplot comparison of **(A)** longitudinal strain ($E_{LL}$)-Delay, **(B)** SD12-$E_{LL}$, and **(C)** longitudinal uniformity ratio estimate (LURE) in normal, narrow QRS (NQRS-HF), and left bundle branch ablation (LBBB-HF) groups is shown.

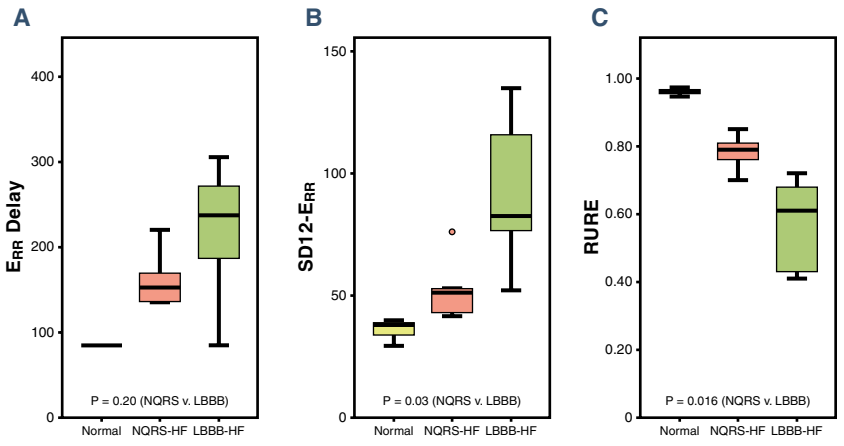


**Figure 4. Boxplots of Radial Dyssynchrony Parameters**

A boxplot comparison of **(A)** radial strain ($E_{RR}$)-Delay, **(B)** SD12-$E_{RR}$, and **(C)** radial uniformity ratio estimate (RURE) in normal, narrow QRS (NQRS-HF), and left bundle branch ablation (LBBB-HF) groups is shown.

control and NQRS-HF groups are similar, whereas the LBBB-HF group demonstrates the greatest amount of dyssynchrony. Median differences and CIs for dyssynchrony parameter differences between the LBBB-HF and normal groups are shown in Table 1.

**Correlations among dyssynchrony metrics.** Only moderate (statistically significant) correlations were present between the FT-based and time-to-peak parameters with $E_{CC}$ and $E_{LL}$ (CURE/SD12-$E_{CC}$: r = −0.62, p = 0.03; LURE/SD12-$E_{LL}$: r = −0.76, p = 0.005). As expected, the correlations were tighter between time-to-peak measures (SD12-$E_{CC}$/$E_{CC}$-Delay: r = 0.95, p < 0.001; SD12-$E_{LL}$/$E_{LL}$-Delay: r = 0.91, p < 0.001; SD12-$E_{RR}$/$E_{RR}$-Delay: r = 0.89, p < 0.001). A

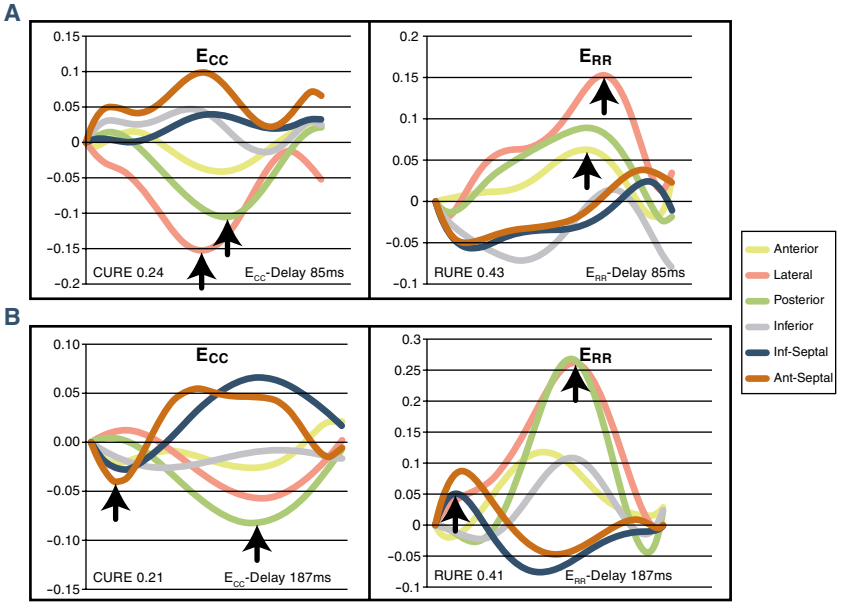


**Figure 5. Comparison of LBBB-HF Dyssynchrony Assessments**

Both cases have significant dyssynchrony due to HF and LBBB. In the first case **(A)**, Fourier transformation (FT)-based measures indicate marked dyssynchrony, but time-to-peak measures do not due to the absence of early contractile strain peaks. In the second case **(B)**, both FT-based and time-to-peak parameters indicate a high level of dyssynchrony. In both cases, both types of time-to-peak parameters (delay and SD12 indexes) resulted in similar assessments. Please see Online Videos 1, 2, 3, and 4. Abbreviations as in Figures 2 to 4.

table with all the correlation data may be found in the Online Appendix.

## DISCUSSION

**Major findings.** The key findings of this study are: 1) cine DENSE provides high-quality dyssynchrony assessments on the basis of circumferential, longitudinal, or radial strain, with good correlation with MTT; 2) cine DENSE assessment of mechanical dyssynchrony in HF with FT-based parameters quantifying the extent of simultaneous myocardial stretch and contraction is feasible; and 3) FT-based dyssynchrony parameters (CURE, RURE, and LURE) derived from CMR effectively discriminate HF with and without LBBB and perform favorably relative to time-to-peak parameters.

**Timing-based versus FT-based dyssynchrony parameters.** Widely used dyssynchrony measures from echocardiography (7,13,14) and CMR published studies (15) are dependent on the time to peak contraction. Despite this, with both echocardiography and CMR, determination of time to peak contraction on the basis of regional tissue velocity or strain curves might be difficult when infarction, akinesis, or dyskinesis is present or when segmental velocity/strain curves have a predominant stretch pattern, low maximal amplitude, and/or multiple peaks. In contrast, FT-based measures such as CURE, LURE, and RURE measure the degree to which some segments contract while other segments stretch during the cardiac cycle and do not require manual identification of strain/velocity peaks, providing an automated and easily interpretable global measure of dyssynchrony. Because these FT-based dyssynchrony parameters can be easily determined with any imaging modality that generates strain curves from standard LV short-axis and long-axis views, this methodology has broad potential clinical applicability.

**Clinical importance of dyssynchrony assessment by echocardiography.** Early single-center echocardiographic studies with tissue Doppler imaging showed that a significant delay between time to peak systolic velocity at basal septal and basal lateral segments predicted a lower adverse clinical event rate after CRT (13). In addition, an alternative parameterization on the basis of the SD of time from QRS onset to peak systolic velocity for 12 LV segments (derived from tissue Doppler imaging) was also shown to be effective and associated with LV reverse remodeling after CRT (14). Subsequently, the multicenter PROSPECT (Predictors of Response to CRT) study "observed relatively low yield and high variability for TDI [tissue Doppler imaging] measures" (5). Although the methodology was criticized by some, the study seemed to have the positive effect of encouraging the development of more advanced echocardiographic dyssynchrony methods with assessments of radial and circumferential strain, such as echo speckle tracking and 3D echocardiography, and positive clinical studies were subsequently published on the basis of these methods (7,8). In addition, advanced strain analysis methods based on myocardial tagging (9) and cine DENSE (11,12) have also been developed for this purpose.

**Clinical impact of refined dyssynchrony imaging.** Despite a large number of CRT-related imaging studies, major guidelines for CRT patient selection in patients with a widened QRS do not include any criteria based on imaging (with the exception of the UK National Institute for Health and Clinical Excellence guidelines) (21). In spite of this, significant heterogeneity in CRT response still exists even in patients with a wide QRS, and there are compelling reasons to improve CRT selection criteria in these patients. These include an increased complication rate associated with CRT-D relative to the rate with standard ICDs. For example, in RAFT (Resynchronization/Defibrillation in Ambulatory Heart Failure Trial), the complication rate for CRT-D was 13%, which was significantly greater than the complication rate for standard ICDs (22). Procedure times and patient radiation exposure are also increased with CRT (23). In addition, CRT carries considerable costs related to the device, implantation, monitoring, and the need for multiple device changes over a lifetime. On the basis of these costs and current CRT nonresponse rates, if the medical community does not develop more effective ways to identify the best CRT candidates, it is possible that reimbursement could be restricted in the future, which could leave a number of potential CRT responders unable to receive this treatment.

In light of recent results for speckle tracking, 3D echocardiography, and CMR modalities such as DENSE and myocardial tagging, it is our opinion that cardiac imaging for mechanical dyssynchrony and viability holds the best promise for developing more meaningful CRT patient selection criteria, although a positive large multicenter randomized trial would be needed to influence guidelines. We believe that effective imaging for mechanical dyssynchrony requires both accurate assessment of cardiac

mechanical function and optimal parameterization of the degree of dyssynchrony. Because the present study has addressed both these issues and demonstrated an advantage for FT-based parameters over time-to-peak parameters, we believe this work will have significant clinical impact. Of note, these FT-based dyssynchrony parameters could have potential broad application to strain data obtained not only from cine DENSE MR but also other imaging modalities capable of generating regional strain curves.

**Limitations and rationale for translational approach.** This is a translational rather than a clinical study, and our model of LBBB might not be representative of all types of mechanical dyssynchrony in human HF; however, this design provided a controlled and validated model to test our hypotheses. Further clinical investigation is indicated on the basis of these data. Of note, we chose a translational approach for several reasons. First, the model was necessary to demonstrate consistency of cine DENSE and MTT for dyssynchrony and strain assessment. Second, the pacing-induced HF model is a well-validated animal model of HF and produces LV dysfunction similar to the LV dysfunction present in patients referred for CRT (1,2). Third, induction of LBBB results in the prototypical model of mechanical dyssynchrony (17) that responds to resynchronization on the basis of prior published data (16). Fourth, the translational model has allowed us to determine that this technique has the potential to perform better than timing-based methods in human HF patients, which justifies further clinical study.

## CONCLUSIONS

Automated FT-based circumferential, radial, and longitudinal dyssynchrony indexes based on heterogeneity of regional segmental strain can be easily determined without the need for time-to-peak contraction determinations and compare favorably with time-to-peak parameters. In the present study, we demonstrate the effectiveness of cine DENSE for this purpose, with validation based on strain obtained from harmonic phase analysis of MTT. Further clinical evaluation is warranted with cine DENSE CMR or other imaging modalities, because this methodology can be extended to any imaging modality capable of generating regional strain curves from standard LV short-axis and long-axis views.

### Acknowledgments

The authors thank Xiaodong Zhong, PhD, Robert Janiczek, PhD, Andrew Gilliam, PhD, John Christopher, RT, and Craig Goodman, BS, for their assistance.

**Reprint requests and correspondence:** Dr. Kenneth Bilchick, University of Virginia Health System, Cardiovascular Division, Post Office Box 800158, Charlottesville, Virginia 22908. *E-mail: bilchick@virginia.edu.*

## REFERENCES

1. Bristow MR, Saxon LA, Boehmer J, et al. Cardiac-resynchronization therapy with or without an implantable defibrillator in advanced chronic heart failure. N Engl J Med 2004;350:2140–50.
2. Abraham WT, Fisher WG, Smith AL, et al. Cardiac resynchronization in chronic heart failure. N Engl J Med 2002;346:1845–53.
3. Cleland JG, Daubert JC, Erdmann E, et al. The effect of cardiac resynchronization on morbidity and mortality in heart failure. N Engl J Med 2005;352:1539–49.
4. Moss AJ, Hall WJ, Cannom DS, et al. Cardiac-resynchronization therapy for the prevention of heart-failure events. N Engl J Med 2009;361:1329–38.
5. Chung ES, Leon AR, Tavazzi L, et al. Results of the Predictors of Response to CRT (PROSPECT) trial. Circulation 2008;117:2608–16.
6. Aiba T, Hesketh GG, Barth AS, et al. Electrophysiological consequences of dyssynchronous heart failure and its restoration by resynchronization therapy. Circulation 2009;119:1220–30.
7. Tanaka H, Nesser HJ, Buck T, et al. Dyssynchrony by speckle-tracking echocardiography and response to cardiac resynchronization therapy: results of the Speckle Tracking and Resynchronization (STAR) study. Eur Heart J 2010;31:1690–700.
8. Marsan NA, Bleeker GB, Ypenburg C, et al. Real-time three-dimensional echocardiography permits quantification of left ventricular mechanical dyssynchrony and predicts acute response to cardiac resynchronization therapy. J Cardiovasc Electrophysiol 2008;19:392–9.
9. Bilchick KC, Dimaano V, Wu KC, et al. Cardiac magnetic resonance assessment of dyssynchrony and myocardial scar predicts function class improvement following cardiac resynchronization therapy. J Am Coll Cardiol Img 2008;1:561–8.
10. Kim D, Gilson WD, Kramer CM, Epstein FH. Myocardial tissue tracking with two-dimensional cine displacement-encoded MR imaging: development and initial evaluation. Radiology 2004;230:862–71.
11. Spottiswoode BS, Zhong X, Hess AT, et al. Tracking myocardial motion from cine DENSE images using spatiotemporal phase unwrapping and temporal fitting. IEEE Trans Med Imaging 2007;26:15–30.
12. Spottiswoode BS, Zhong X, Lorenz CH, Mayosi BM, Meintjes EM, Epstein FH. Motion-guided segmentation for cine DENSE MRI. Med Image Anal 2009;13:105–15.
13. Bax JJ, Bleeker GB, Marwick TH, et al. Left ventricular dyssynchrony predicts response and prognosis after cardiac resynchronization therapy. J Am Coll Cardiol 2004;44:1834–40.

14. Yu CM, Fung JW, Zhang Q, et al. Tissue Doppler imaging is superior to strain rate imaging and postsystolic shortening on the prediction of reverse remodeling in both ischemic and nonischemic heart failure after cardiac resynchronization therapy. Circulation 2004;110:66–73.
15. Westenberg JJ, Lamb HJ, van der Geest RJ, et al. Assessment of left ventricular dyssynchrony in patients with conduction delay and idiopathic dilated cardiomyopathy: head-to-head comparison between tissue Doppler imaging and velocity-encoded magnetic resonance imaging. J Am Coll Cardiol 2006;47:2042–8.
16. Leclercq C, Faris O, Tunin R, et al. Systolic improvement and mechanical resynchronization does not require electrical synchrony in the dilated failing heart with left bundle-branch block. Circulation 2002;106:1760–3.
17. Bilchick KC, Helm RH, Kass DA. Physiology of biventricular pacing. Curr Cardiol Rep 2007;9:358–65.
18. Zhong X, Spottiswoode BS, Meyer CH, Kramer CM, Epstein FH. Imaging three-dimensional myocardial mechanics using navigator-gated volumetric spiral cine DENSE MRI. Magn Reson Med 2010;64:1089–97.
19. Zerhouni EA, Parish DM, Rogers WJ, Yang A, Shapiro EP. Tagging with MR imaging—a method for noninvasive assessment of myocardial motion. Radiology 1988;169:59–63.
20. Moore CC, Lugo-Olivieri CH, McVeigh ER, Zerhouni EA. Three-dimensional systolic strain patterns in the normal human left ventricle: characterization with tagged MR imaging. Radiology 2000;214:453–66.
21. UK National Institute for Health and Clinical Excellence. TA120 Heart failure—Cardiac Resynchronisation: Guidance. July 2010. Available at: http://guidance.nice.org.uk/TA120/Guidance/pdf/English. Accessed November 1, 2011.
22. Tang AS, Wells GA, Talajic M, et al. Cardiac-resynchronization therapy for mild-to-moderate heart failure. N Engl J Med 2010;363:2385–95.
23. Perisinakis K, Theocharopoulos N, Damilakis J, Manios E, Vardas P, Gourtsoyiannis N. Fluoroscopically guided implantation of modern cardiac resynchronization devices: radiation burden to the patient and associated risks. J Am Coll Cardiol 2005;46:2335–9.

**Key Words:** cardiac magnetic resonance ■ cardiac resynchronization therapy ■ heart failure.

## APPENDIX

**For supplementary figures and videos, please see the online version of this article.**